ISSN 1995-4212, Polymer Science, Series D. Glues and Sealing Materials, 2015, Vol. 8, No. 2, pp. 100–109. © Pleiades Publishing, Ltd., 2015.
Original Russian Text © A.A. Olkhov, O.V. Staroverova, A.P. Bonartsev, I.I. Zharkova, E.D. Sklyanchuk, A.L. Iordanskii, S.Z. Rogovina, A.A. Berlin, A.A. Ishchenko, 2014, published in Vse Materialy. Entsiklopedicheskii Spravochnik, 2014, No. 12, pp. 2–13.

# Structure and Properties of Ultrathin Poly-(3-Hydroxybutirate) Fibers Modified by Silicon and Titanium Dioxide Particles

**A. A. Olkhov[a], O. V. Staroverova[b], A. P. Bonartsev[c], I. I. Zharkova[c], E. D. Sklyanchuk[d], A. L. Iordanskii[b], S. Z. Rogovina[b], A. A. Berlin[b], and A. A. Ishchenko[e]**

[a] *Russian Institute of Economics, Moscow, Russia*
[b] *Institute of Physical Chemistry of the Russian Academy of Sciences, Moscow, Russia*
[c] *Moscow State University, Moscow, Russia*
[d] *Clinical Hospital of the Russian Railways, Moscow, Russia*
[e] *Moscow State University of Thin Chemical Technologies, Moscow, Russia*
*e-mail: aolkhov72@yandex.ru*

Received August 11, 2014

**Abstract**—The influence of small concentrations of nanoscale silicon and titanium dioxide particles on the structure, physicomechanical and sorption properties, thermal destruction resistance, and thermal and photo oxidant destruction of unwoven ultrathin fibrous materials that are prepared via electrostatic solution spinning is studied. It is established that nanoscale particles favor the formation of thinner fibers with improved physical and mechanical parameters; good resistance to thermal, thermo- and photo oxidant destruction; and positive dynamics of mesenchymal stem cells.

*Keywords*: ultrathin fibers, poly-(3-hydroxybutirate), nanoscale silicon, nanoscale titanium dioxide, electric spinning, thermal oxidation, thermal destruction, photo oxidation, mechanical properties, mesenchymal stem cells

**DOI:** 10.1134/S1995421215020124

## INTRODUCTION

In the present day, various constructions of polymeric materials prepared via the promising method of electrostatic spinning (ES) of nanocomposite fiber materials based on biopolymers are widely used in tissue engineering [1–3]. This method allows one to obtain fibrous structures with a large surface area to volume ratio, which favors conditions for free migration and proliferation of cells in the three-dimensional space of a matrix and, correspondingly, a high level of integral ability of material in the living tissues of the organism [4].

Among polymers, polyoxyalcanoates (POA) occupy a special place, and poly-(3-hydroxybutirate) (PHB) is the most widely used polymer [5, 6]. This polymer, which is synthesized via the biotechnological method, exhibits such promising properties as high level of biocompatibility [7–9] and biodecomposition ability in living tissues without the formation of toxic products [10–12]. For this reason, PHB is widely studied and used for the development of a whole series of medical instruments for surgery, dentistry, cardiosurgery, orthopedics, and other fields [13, 14].

The physicochemical characteristics, diffusion properties, and kinetics of oxidation, photooxidation, and biodegradation of fibrous unwoven materials are affected by the average diameter of a single fiber and its molecular and supramolecular structure [7]. The diameter of ES fibers depends on such parameters as the concentration of material in the initial solution, the dissolvent evaporation rate, the voltage, the distance from a capillary to the forming layer, the electric conductivity, the viscosity, the temperature, and so on [4]. Thereby, obtaining fibers with a specific morphology is one of the main problems at present.

However, in the case of PHB, changes in the technological parameters of electric spinning (electric conductivity, performance, viscosity of the forming solution) exert almost no influence on the diameter of ultrathin fibers [15, 16]. Thereby, the structure and properties of PHB unwoven material will be almost unchanged.

In connection with the tasks of developing modern bioresorbable fibrous materials for their application as matrices for delivery of controlled doses of medication or for growing living cells, artificial ligament prostheses, and so on, it is important to have a method allowing variation of the structural parameters of PHB fibers for the construction of materials with required characteristics.

It is known that the introduction of nanoscale additives of various natures into the polymers leads to signif-

icant modification of structural parameters and, correspondingly, of the material properties [15, 17–19].

The present work is thus aimed at studying the influence of nanoscale titanium dioxide and silicon particles on structure and properties of PHB ultrathin fibers.

Poly-(3-hydroxybutirate) (PHB) with a molecular mass of 300 and 460 kDa (BIOMER Corp., Germany) in the form of powder prepared via microbiological synthesis and domestically produced CP reactives, such as chloroform (CF), formic acid (FA), and tetrabutylammonium iodide (TBAI). Titanium dioxide of two modifications (η-$TiO_2$ and $TiO_2$ (anatase)) synthesized at the Department of Solid State Physics and Chemistry of the Moscow State University of Thin Chemical Technologies and nanocrystalline silicon with a composition nc-Si/protective shell with a nanosilicon nucleus diameter of 1.5–3.5 nm were used as the modifying additives [17].

Nanoscale titanium dioxide modifications with anatase and η-$TiO_2$ structure were synthesized via the sulfate method using two pristine reagents $(TiO)SO_4 \cdot xH_2SO_4 \cdot yH_2O$ (I) and $(TiO)SO_4 \cdot 2H_2O$ (II) [20].

Tetrabutylammonium iodide $\{[CH_3(CH_2)_3]_4N\}$ was used in the process of electric spinning as an additive for increasing electric conductivity of the forming solution and, thus, for removing morphological defects in fibers, so-called pears. Formic acid was added for regulating viscosity and electric conductivity.

ES of unwoven PHB fibrous materials was made on an experimental laboratory system [2, 4] at a dynamic solution viscosity of 2–9 P, specific bulk conductivity of $\sim 10^{-3}$ $(\Omega\ m)^{-1}$, volume flow of the forming solution of $10–12 \times 10^{-5}$ g/s, electric field voltage of 15 kV, and distance between the electrodes of 18 cm.

The PHB fiber distribution in CF/FA (0.9 : 0.1) with TBAI in accordance with the diameters was studied via light and electron microscopy (an MBI-6 optical microscope and Hitachi TM-1000 scanning electron microscope). Thermophysical and thermal characteristics (the thermal and thermooxidative destruction onset temperatures) of PHB fibers are obtained via DSM-2 (Russia) and Perkin Elmer Pyris 6 DSC (United States) differential scanning calorimeters.

The strength of PHB fibrous materials was probed on an RM-3-1 tensile testing machine in accordance with TC 25.061065–72 using samples with a size of $4 \times 1$ cm$^2$ cut from the unwoven fibrous material which was formed for 1.5 h by means of the formula $L = L = \left(F\frac{l_0}{m}\right) \times 100$, where $F$ is the breaking load, N; $l_0$ is the initial length of the sample between clamps, m; and $m$ is the mass of the sample between clamps, g.

The kinetics of UV aging was studied on the same samples utilizing a Feutron 1001 artificial weathering chamber (Germany) equipped with a UV source—a high-pressure mercury lamp with a power of 385 W.

The distance from the lamp to the samples was 30 cm [21].

The molecular mobility was investigated via microprobe EPMR. A stable 2,2,6,6- tetramethylpiperidine-1-oxyl (TMPO) nitroxyl radical was used as the probe. It was introduced into the fibrous material from vapor at 250°C to attain a concentration not exceeding $10^{-3}$ mol/L. EPMR spectra were registered in the absence of saturation, which was verified via the dependence of signal intensity on microwave field power. Probe rotation correlation time values τ were determined from EPMR spectra using the formula [22] $\tau = \Delta H^+(\sqrt{I^+/I^- - 1})\ 6.62 \times 10^{-10}$ where $\Delta H^+$ is the spectral component width in the weak field and $I^+/I^-$ is the component intensity in the weak and in the strong fields, respectively. The error in τ calculation was ±5%.

Birefringence value $\Delta n$ was measured by an MPD-1 polarization optical microscope (Russia) [23]. Prepared samples of unwoven PHB fibrous materials with added titanium oxide (samples 1–5) were probed via X-ray diffraction: HZG-4 (Ni-filter) and DRON-3M (graphite plate monochromator) diffractometers on Cu$K_\alpha$ radiation (reflection registration; sample rotation, step-by-step regime: pulse set time is 10 s, and the step is 0.02°). Experimental data were processed using the PROFILE FITTING V 4.0 software. Qualitative phase analysis of samples was carried out utilizing the JCPDS PDF-2 database, ICSD structural database, and the original papers. The coherent domain (CD) sizes, which are usually considered to be equal to the crystallite sizes [24], were evaluated in accordance with the Debye–Scherer formula $D = \frac{k\lambda}{\beta \cos\theta_{hkl}}$, where β is the width at the half-height of the peak for the studied phase, $k \sim 0.9$ is the empirical coefficient, and λ is the wavelength. To calculate the CD in the dioxide, the strongest reflections at $2\theta \sim 25°$ for both anatase and η-$TiO_2$, and at $2\theta \sim 22°$ for $TiO_2$/opal composite were used. The standard error was ±5%.

The water vapor sorption and desorption by unwoven fibrous materials was studied by gravimetry at a temperature of 23°C.

In order to determine the biocompatibility of polymeric matrices, cell cultivation on the matrix surface was used. For this purpose, mesenchymal stem cells (MSC) from human adipose tissue (Biolot, Russia) were used. The cells were cultivated in DMEM (Dubecco's Modified Eagle Medium, Invitrogen, United States) with increased glucose content (4.5 g/L) containing 10% fetal calf serum (FCS),

**Table 1.** Average diameter and mechanical characteristics of fibers as functions of PHB mass and forming solution concentration

| Composition | Average diameter, nm | Breaking length, m | Relative extension, % |
|---|---|---|---|
| 5% PHB (460 kDa) in CF | 2550 | 211 | 23 |
| 7% PHB (460 kDa) in CF | 2750 | 586 | 19 |
| 9% PHB (460 kDa) in CF | 3400 | 820 | 17 |
| 7% PHB (300 kDa) in CF | 2850 | 416 | 7 |

100 mol. eq./mL penicillin, and 100 μg/mL streptomycin (Invitrogen, United States). The cells were incubated at 37°C in an atmosphere with 5% of $CO_2$ that was changed every 3 days. Fibroblasts were taken from the substrate by the trypsin–EDTA (versen) solution (0.05% trypsin and 0.02% EDTA in phosphate saline buffer (PSB) (Serva, Germany)) and calculated by means of a Goryaev's chamber.

Eight samples of each matrix with a size of $5 \times 5$ mm$^2$ were placed in the wells of a tablet with 96 wells, and the cell suspension was deposited onto each sample in a quantity of 5000 cells per matrix. The tablets were then incubated for 1, 3, 4, and 8 days.

The survival and proliferation of cells were controlled via a test based on the reaction of transformation of an insoluble tetrazolium salt into a soluble colored formazan salt implemented via active mitochondrial cell ferments (XTT Cell Proliferation Kit, Biological Industries, Israel). Measurements were carried out on a Zenyth 3100 Microplate Multimode Detector (Anthos Labtec Instruments GmbH, Austria) tablet spectrophotometer at a wavelength of 450 vs. 620 nm. The amount of living cells was determined via a standard calibration straight line for the SSC test [7].

In order to prepare the forming solution with optimum conductivity, viscosity, molecular mass of polymer, and polymer concentration, we carried out corresponding research.

Earlier, we have already investigated the effect of conductivity and viscosity on ES of PHB fibers [15, 25]. It was established that conductivity of PHB solution in CF is not sufficient for ES. For this reason, to increase conductivity, 5 g/L of TBAI was introduced into the solution. To reduce the salt content in the solution, FC was added in the ratio to chloroform of 1 : 10. TBAI concentration decreased by five times.

It was found that ES is stable in the PHB forming solution content range of from 2 to 18 P.

The following step was to determine the optimum PHB molecular mass for the fabrication of fibrous materials. For comparison, PHB with two molecular masses—300 and 460 kDa—which are most used in the formation of film and fibrous materials, were used.

The average diameters of fibers were found from SEM optical micrographs (see Fig. 1 and Table 1).

As is obvious from the data, the PHB molecular mass exerts almost no influence on the average fiber diameter. The mechanical characteristics are higher for unwoven PHB fibrous materials with a molecular mass of 460 kDa. For further investigations, PHBs with a molecular mass of 460 kDa were chosen.

The influence of PHB solution concentration was further explored. It is obvious from Fig. 1 (a–c) and Table 1 that the increasing viscosity of the forming solution favors a slight growth of the average fiber diameter. Herewith, with growing PHB content, the breaking length increases and the relative elongation of fibers slightly decreases.

This effect is evidently due to the kinetics of PHB crystallization during microfiber formation (the amorphous to crystalline phase ratio, and the presence of dense and more loosened sites in the amorphous zone). As follows from DSC data, the degree of crystallinity of pristine PHB (a powder) was 69%, while for a fibrous material from a 7% solution it attained 73%.

Note that, if, in the development of fibrous sensors, decreasing the fiber diameter to the nanoscale range is the main thing that needs to be done to improve their sensibility, in the case of biomedical application of fibrous materials—for example, in the fabrication of porous matrices for cell engineering—such a decrease in the fiber diameter leads to poor adhesion of cells and reduces their growth rate [14, 25].

The possibility of controlling the geometry of ultrathin fiber via modification of physicochemical characteristics of the solution has been described in recent works [26]. In our case, 7% PHB forming solution was chosen for our manipulations as the basic material due to the well-recovered physicochemical characteristics and fiber geometry obtained from this solution. For this reason, subsequent measurements

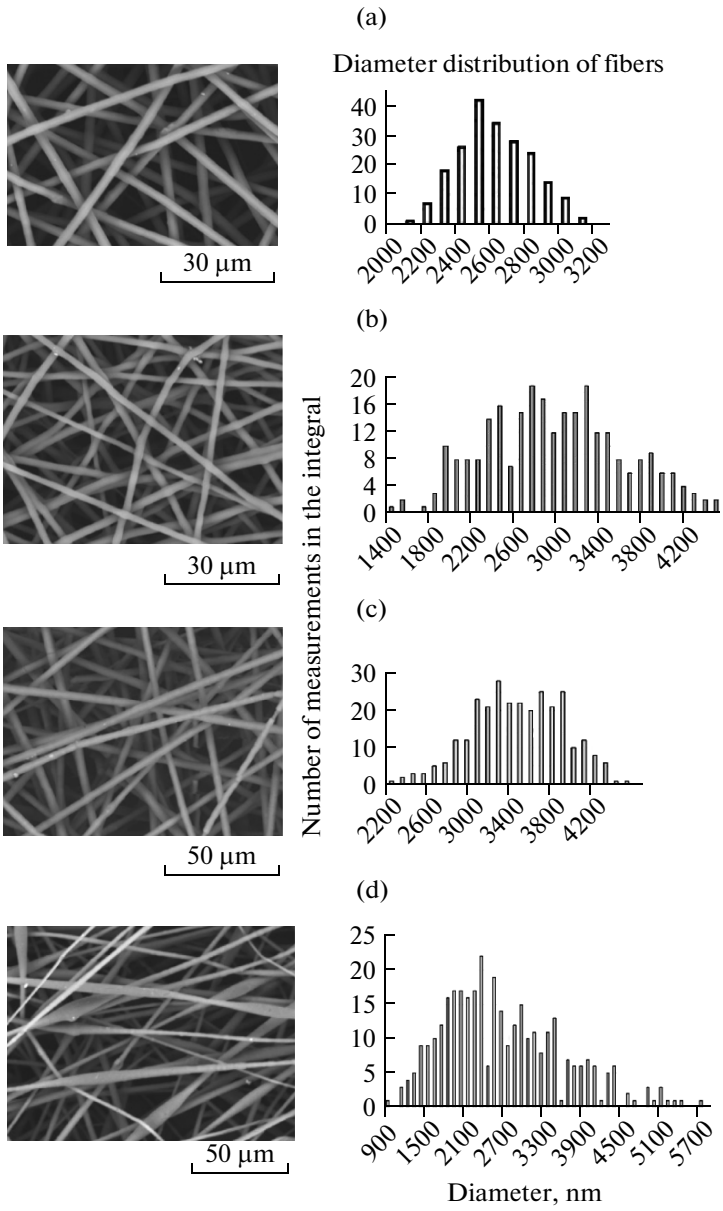


**Fig. 1.** Electron microscopy optical images and the diameter distribution of fibers for (a) 5% PHB solution in CF, (b) 7% PHB solution in CF, (c) 9% PHB solution in CF, and (d) 7% PHB solution (300 kDa) in CF.

were made taking into account these properties, as well as based on the conducted experiments on the determination of physicomechanical characteristics and the average fiber diameter.

The fiber structure was probed via birefringence. A polarization optical microscope allowed obtaining a poorly resolved image of a so-called Maltese cross, this testifying to the presence of anisotropy of macromolecules in PHB fibers. Unfortunately, a quantitative determine of the orientation factor was not available because of the lack of unidirectional filament stacking in the unwoven material.

X-ray profile of the unwoven PHB material is shown in Fig. 2. Using the Wolf–Bragg equation, interplane distance $d$ was caclucated:

$$\frac{2\sin\Theta}{\lambda} = \frac{1}{d},$$

where $\Theta$ is the diffraction angle, deg, and $\lambda$ is the wavelength equal to 1.54051 nm.

It is seen from Fig. 2 and Table 2 that the interplane distances in PHB crystallites are almost the same for both isotropic PHB film deposited onto a glass substrate from 7% solution and ES fibers. The degrees of

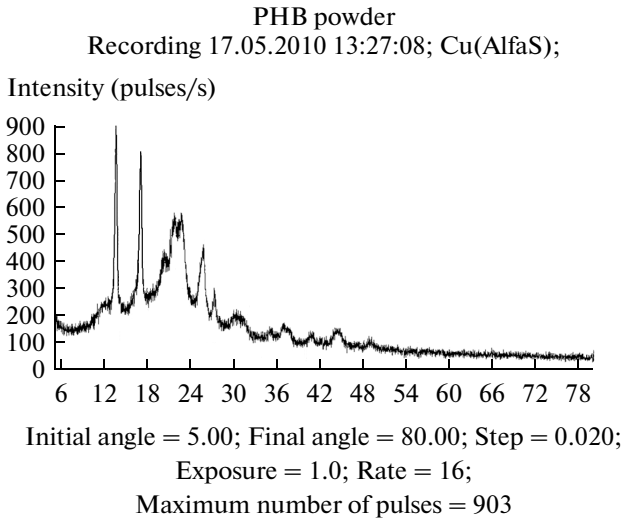


**Fig. 2.** X-ray diffraction profiles of unwoven PHB material formed of 7% PHB solution in CF.

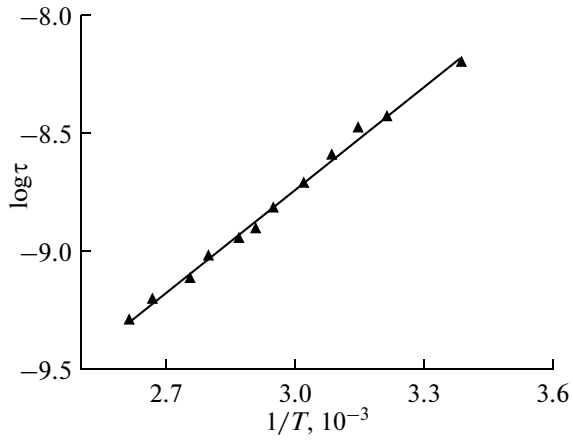


**Fig. 3.** Correlation time as a function of the inverse temperature for the fibrous matrix.

crystallinity and the melting points of samples are almost equal as well. This may testify to the identity of the crystalline PHB structure for both isotropic polymer and ES fibers.

To study the structure of the amorphous phase in fibers, we used microprobe EPMR spectroscopy, which allows determining not only the dynamic characteristics of segment movement, but also the differences in densities of the amorphous phase, being a combination of more or less ordered sites.

EPMR spectra of matrices based on PHB fibers are a superposition of two individual spectra from radicals with different correlation times that characterize the molecular mobility in more-or-less dense amorphous sites of a polymer. The presence of at least two radical correlation times in the amorphous zone of PHB fibrous matrices indicates that the intercrystalline polymer zones have a heterophase structure and coincides with the modern twin-phase model of the amorphous state of crystallizing polymers that is applied to partially crystallized polyethers, such as PHB, polylactide, and polyethylene terephtalate [27].

In addition to dynamic measurements, a sorption experiment is used for determination of the quantity of a radical adsorbed in the fiber material sample. Calculation based on spectrum integration revealed $0.23 \times 10^{17}$ radicals in the fiber.

Using the technique for calculation of the correlation times, their temperature dependencies, which enable us to determine the activation energies of the rotational mobility of the radical in the studied polymeric samples, were obtained (Fig. 3). According to the calculations, this value is 42 kJ/mol in the fiber.

Thereby, EPMR spectral analysis revealed that the intercrystalline sites (of the amorphous phase) in fibrous material samples have various degrees of structural organization.

We have also studied the influence of nanoscale modifiers (titanium dioxide and silicon) on the properties of unwoven PHB fibrous materials.

Via an ultrasonic bath, 0.01% of nanoscale particles were introduced into the polymer solution immediately before electrostatic spinning.

IResearch and development are actively taking place in the areas of synthesis, characterization, and analysis of nanosilicon, silicon carbide, and titanium dioxide, as well as synthesis and characterization of the physicochemical properties of hybrid photoactive silicon-based structures, including organic and inorganic emulsion materials, hydrogels, and UV protective and photoluminescent polymeric materials [15, 20, 28–30]. The importance of this research is proven by the practical significance of the anticpated results.

**Table 2.** Melting point $T_{melt}$, degree of crystallinity (DSC) $\alpha_{cr}$, and interplane distances of characteristic peaks (according to the X-ray diffraction profile) for PHB in pristine polymer and in fibers

| Sample | $\Theta_1$ | $d_1$ | $\Theta_2$ | $d_2$ | $\Theta_3$ | $d_3$ | $T_{melt}$, °C | $\alpha_{cr}$, % |
|---|---|---|---|---|---|---|---|---|
| PHB film | 6.8 | 1.5588 | 8.65 | 1.10102 | 13.7 | 0.87163 | 175 | 75 |
| PHB fibers | 6.8 | 1.5588 | 8.5 | 0.96461 | 13.6 | 0.89648 | 177 | 73 |

**Table 3.** The influence of silicon and titanium dioxide nanoparticles on the average diameter, characteristics, and sorption properties of PHB fibers

| Sample | $D_{av}$ | $L_p$ | $\varepsilon_p$ | $s_v$ | $V_s$ |
|---|---|---|---|---|---|
| PHB fiber | 2750 | 586 | 19 | 1.2 | 2 |
| PHB fiber with $TiO_2$ (anatase) | 1100 | 1500 | 80 | 2.4 | 4 |
| PHB fiber with η $TiO_2$ | 1400 | 1000 | 32 | 2.2 | 5 |
| PHB fiber with nc-Si | 850 | 1795 | 31 | 1.9 | 8 |

$D_{av}$ is the average diameter, nm; $L_p$ is the breaking length, m; $\varepsilon_p$ is the relative extension, %; $s_v$ is the water desorption rate, g/min; and $V_s$ is the sorption capacity for water vapor per 400 h, g/g.

**Table 4.** Thermophysical characteristics pf PHB fibers with nanoparticles and the onset temperature of thermal destruction and thermooxidative destruction

| Sample | $T_{melt}$, °C | $T_{cr}$, °C | χ, % | $E_{melt}$ | $T^{T}_{onset}$ | $T^{TO}_{onset}$ |
|---|---|---|---|---|---|---|
| PHB fibers | 177 | 74 | 73 | 0,75 | 231 | 288 |
| PHB fibers with $TiO_2$ (anatase) | 178 | 68 | 72 | 0,55 | 243 | 321 |
| PHB fibers with η$TiO_2$ | 177 | 69 | 72 | 0,65 | 239 | 295 |
| PHB fibers with nc-Si | 179 | 67 | 71 | 0,6 | 240 | 302 |

$T_{melt}$ is the melting point, °C; $T_{cr}$ is the crystallization point, °C; χ is the degree of crystallinity (DSC), %; $E_{melt}$ is the melting activation energy, MJ/K; $T^{T}_{onset}$ is the onset temperature of the thermal destruction, °C; and $T^{TO}_{onset}$ is the onset temperature of thermooxidative destruction, °C.

The introduction of small nanoparticle concentrations, it is believed, will affect the kinetics of PHB crystallization and thus modify the supramolecular structure of the synthesized thin fibers. At the same time, both the diameter and physicomechanical characteristics of a fiber must be changed.

As is seen from Table 3, introducing silicon and titanium dioxide nanoparticles into the forming solution led to a decrease in the average fiber diameter by two to three times in comparison with the initial value. Herewith, the physicomechanical indices grew by 1.5–3 times. The smallest diameter and the highest physicomechanical indices were observed for fibrous materials modified by silicon nanoparticles.

Comparison of the parameters of fibers with two different titanium dioxide nanoparticle modifications revealed that the smallest diameter and better physicomechanical properties are typical of fibers containing anatase titanium dioxide particles.

In studying the fiber materials via differential scanning calorimetry (Table 4), it was found that the melting point of PHB was almost unchanged in the presence of nanoparticles, while the crystallization temperature in the modified fibers falls by 5–7°C. The degree of polymer crystallinity is almost constant.

In comparing the physicomechanical and calorimetrical data, one can confirm that silicon and titanium dioxide nanoscale particles have an effect on the PHB structure in the solution and on the supramolecular organization of polymeric chains in the forming ultrathin fiber.

As is seen in Table 4, adding nanoparticles with high specific surface and chemical activity [31] to the polymeric fiber leads to acceleration of polymer–matrix crystallization and to a decrease in the activation energy during polymeric phase melitng.

Silicon and titanium dioxide behave in a polymer solution (as in the melt) as crystallization seeds.

Thereby, upon electrostatic spinning of the polymeric solution, the nanoparticles accelerate the formation of a supramolecular PHB structure. It can be supposed that the increase in physicochemical indices of fibrous materials in the presence of silicon and titanium dioxide nanoparticles is the result of the accelerating processes of orientated PHB crystallization in the field of tensile forces in the formation of a primary flow of the forming solution [4]. Herewith, a more ordered supramolecular PHB structure is formed.

Physicomechanical tests reveal that the introduction of small concentrations of nanoscale particles modifies the properties of fibrous material significantly. The mechanics of stretching of unwoven fibrous material being layers of ultrathin fibers (Fig. 1) is indeed the stripping and the gradual straightening of fibers (at the initial stage), while, at the final stage of deformation, a single fiber (more precisely, its structure) contributes the strain and strength characteristics; i.e., there are two simultaneous processes:

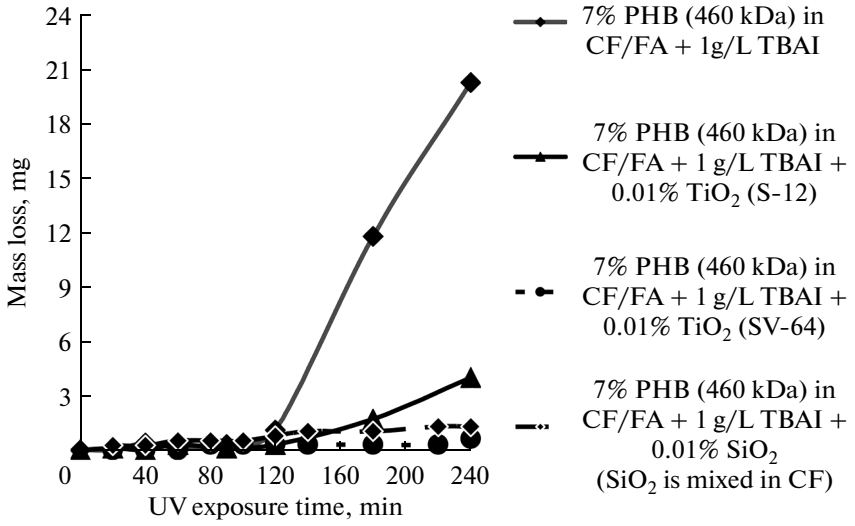


**Fig. 4.** Mass loss by unwoven fiber samples as a function of UV exposure time.

straightening of fibers and deformation of straightened fibers.

In this work, the influence was studied of small concentrations of nanoscale silicon and titanium dioxide particles on the thermal and thermooxidative destruction resistance of fibrous materials (in inert medium) (Table 4). As is obvious from the data, the introduction into PHB fibers of small concentrations of nanoscale silicon and titanium dioxide particles leads to the formation of a more ordered supramolecular PHB structure with a higher resistance to thermal and thermooxidant destruction. As is known from the scientific literature, increased resistance to thermal oxidation and thermal destruction is typical of polymeric oriented materials [32].

Studies of the resistance for PHB fibers modified by silicon and titanium dioxide nanoparticles revealed that the latter favor a considerable increase in the UV resistance of PHB fibers (Fig. 4). As is seen from Fig. 4, UV radiation of samples leads to massive losses in the fibrous material. It is known from the references that UV aging provokes the release of a large amount of gaseous products. We can assume that, during UV aging of fibrous PHB materials, carbon dioxide and water are mainly released.

It is seen from the data in Fig. 4 and Table 5 that, in the presence of UB radiation for 240 min, the destruction of ultrathin fibers is rather deep, going all the way to crystalline phase damage, which is proven by the

**Table 5.** Melting point, degree of crystallinity, and onset temperature of thermal destruction of PHB fibers

| Sample | $T_{melt}$, °C | | χ | | $T^{T}_{onset}$ | |
|---|---|---|---|---|---|---|
| | pristine | after UV | pristine | after UV | pristine | after UV |
| PHB fibers | 174 | 166 | 73 | 6 | 239 | 226 |
| PHB fibers with nc-S | 179 | 165 | 71 | 20 | 240 | 210 |
| PHB fibers with $hTiO_2$ | 177 | 160 | 72 | 10 | 231 | 208 |
| PHB fibers with $TiO_2$ (anatase) | 178 | 167 | 72 | 12 | 243 | 215 |

UV radiation for 240 min; $T_{melt}$ is the melting point, °C; χ, is the degree of crystallinity (DSC), %; and $T^{T}_{onset}$ is the onset temperature of thermal destruction, °C.

significant decrease in the degree of crystallinity and the melting point. The decreasing melting point also indicates the appearance of defective crystallites in PHB.

The decrease in the thermal destruction onset temperature of UV-irradiated fibrous materials also indicates partial amorphization of PHB phase sites and the emergence of defective crystallites.

Herewith, PHB fibers with nanoscale silicon and titanium dioxide particles exhibit a larger resistance to photoinduced oxidation than do pristine fivers. As is seen from Table 5, the degree of crystallinity of the modified fibers after UV aging is approximately two to three times higher than for with the pristine fibers. This testifies to a more ordered crystalline structure and the presence of denser (oriented) formations in amorphous (intercrystalline) PHB sites that are formed due to the influence of nanoscale silicon and titanium particles. Dense amorphous zones in PHB fibers were earlier detected by EPMR.

Sorption characteristics of unwoven fibrous materials are shown in Table 3. The fibers modified by silicon and titanium dioxide adsorb water more intensely than do pristine fibers. The study of an ultrathin fiber surface via electron microscopy revealed nanoscale pores on the surface of fibers with modifying additives (Fig. 5). Due to a such morphology, the fibrous materials modified by nanoparticles exhibit a higher sorption capacity.

As was found from our investigations, the nanoscale surface pores exert no influence on the mechanical properties, but do on the sorption ones. It is clear from the results of the study of MSC on the surface of polymeric matrices by the SSC test (Table 6) that the cell growth is greatest on the fourth day on unwoven samples modified by nanoscale additives.

The best biocompatibility thatw as found from cell growth intensity was found in matrices with nanoscale silicon. Interestingly, these matrices have the smallest filament diameter and, consequently, their physicochemical properties are significantly different from those of others: in particular, these matrices are much more plastic. Moreover, the presence of such additives in these matrices as tetrabutylammonium iodide, nanoscale anatase titanium dioxide, $\eta$-$TiO_2$, and silicon did not affect the growth of cells. For this reason, it can be assumed that MSC cell growth on the matrices prepared via electrospinning is mostly affected by their morphology—in particular, by the diameter of threads which form the matrix, and by the ultrathin fiber surface. MSC cells grow well on the polymeric films with the average roughness [33].

Taking into account the large density of a packing of matrices prepared with the addition of TBAI and titanium oxide [14], MSC cells can be assumed to not be attached to individual matrix threads, but to grow on a network of a few or many threads. It is probable that MSC cells perceive this network of thin filaments as a monolithic rough surface, while the thick filaments and the smaller density of the additive-free stacked matrices force the cells to attach to the individual filaments, at the intersection of or in close proximity to threads, which greatly inhibits their growth. For this reason, matrices prepared via electric spinning of the forming PHB solutions modified by silicon and titanium dioxide nanoparticles can be recommended for growing VSC with a view to their application in tissue engineering.

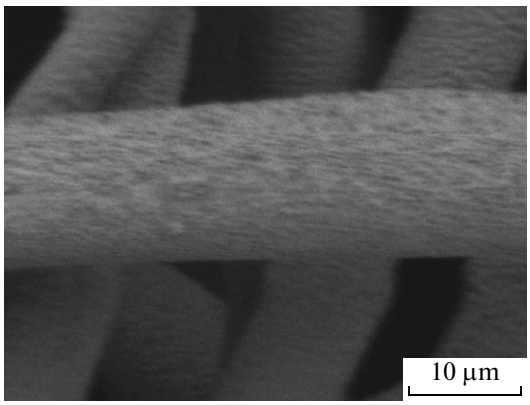


**Fig. 5.** Image of PHB fiber with nanoscale silicon particles.

**Table 6.** Data on the dynamics of mesenchymal stem cells (MSCs) for different PHB samples

| Sample | Cell concentration per mL, $10^3$ | | |
|---|---|---|---|
| | 24 h | 72 h | 96 h |
| PHB fibers | 40 | 175 | 130 |
| PHB fibers with $TiO_2$ (anatase) | 30 | 148 | 220 |
| PHB fibers with $\eta TiO_2$ | 65 | 235 | 248 |
| PHB fibers with nc-Si | 75 | 245 | 270 |

## CONCLUSIONS

(i) The structure of the PHB crystalline phase is almost identical in both isotropic polymer and ES fibers.

(ii) Analysis of EPMR spectra revealed that samples of fibrous material have intercrystalline sites with various degrees of structural organization.

(iii) PHB fibrous materials with a small concentration of silicon and titanium dioxide nanoparticles are characterized by the smallest single fiber diameters and increased physicomechanical parameters.

(iv) Nanoscale silicon and titanium dioxide particles favor the formation of an ordered supramolecular structure in PHB fibers that is resistant to thermal destruction and thermal oxidation.

(v) Ultrathin fibers with nanoparticles have nanoscale surface pores.

(vi) The structures of filaments with a smaller diameter and a higher density form the most favorable basis for MSC cell growth.

(vii) Silicon nanoparticleshave the greatest influence on the structure and properties of ultrathin PHB fibers.

## ACKNOWLEDGMENTS

This work was supported within the Program of Fundamental Research by DCSM-1 (2014) "Production of Macromolecular New Generation Structures" and by the Russian Foundation for Basic Research, projects nos.14-03-00405-a and 13-02-12407ofi_m2.

## REFERENCES

1 1. A. Greiner and J. H. Wendorff, Adv. Polym. Sci., 107–171 (2008).

2. Y. Filatov, A. Budyka, and V. Kirichenko, *Electrospinning of Micro- and Nanofibers: Fundamentals in Separation and Filtration Processes* (Begell House Inc, New York, 2007).

3. A. Kulkarni, V. A. Bambole, and P. A. Mahanwar, Polymer-Plastics Technol. Engin., No. (5), 427–441 (2010).

4. Yu. N. Filatov, *Electrospinning of Fibrous Materials (ESF process)* (Neft' i Gaz, Moscow, 1997) [in Russian].

5. A. P. Bonartsev, S. G. Yakovlev, E. V. Filatova, G. M. Soboleva, T. K. Makhina, G. A. Bonartseva, K. V. Shaitan, V. O. Popov, and M. P. Kirpichnikov, Biochemistry (Moscow) Suppl. Ser. B: Biomed. Chem., No. (1), 42–47 (2012).

6. A. P. Bonartsev, A. L. Iordanskii, G. A. Bonartseva, and G. E. Zaikov, J. Balkan Tribol. Assoc. **14** (3), 359–395 (2008).

7. I. I. Zharkova, A. P. Bonartsev, A. P. Boskhomdzhiev, Yu. M. Efremov, D. V. Bagrov, T. K. Makhina, V. L. Myshkina, E. A. Ivanov, V. V. Voinova, S. G. Yakovlev, A. L. Zernov, E. V. Filatova, N. V. Andreeva, G. A. Bonartseva, and K. V. Shaitan, Biomed. Khim. **58** (5), 579–591 (2012).

8. Yu. N. Pankova, A. N. Shchegolikhin, A. L. Iordanskii, A. L. Zhulkina, A. A. Olkhov, and G. E. Zaikov, "The characterization of novel biodegradable blends based on polyhydroxybutyrate: the role of water transport," J. Mol. Liquids **156** (1), 65–69 (2010).

9. A. A. Ol'khov, A. L. Iordanskii, S. V. Vlasov, R. Yu. Kosenko, Yu. S. Simonova, and G. E. Zaikov, "Matrices of furatsilina controlled release based on films made of polyhydroxybutyrate modified with shungite," Entsikl. Inzhenera-Khimika, No. 7, 17–21 (2012).

10. A. P. Boskhomdzhiev, A. P. Bonartsev, T. K. Makhina, V. L. Myshkina, E. A. Ivanov, D. V. Bagrov, E. V. Filatova, A. L. Iordanski, and G. A. Bonartseva, Biochemistry (Moscow) Suppl. Ser. B: Biomed. Chem. **4** (2), 177–183 (2010).

11. A. P. Bonartsev, A. P. Boskhomodgiev, A. L. Iordanskii, G. A. Bonartseva, A. V. Rebrov, T. K. Makhina, V. L. Myshkina, S. A. Yakovlev, E. A. Filatova, E. A. Ivanov, D. V. Bagrov, and G. E. Zaikov, Mol. Crystals Liquid Crystals **556** (1), 288–300 (2012).

12. A. P. Bonartsev, A. P. Boskhomodgiev, V. V. Voinova, T. K. Makhina, V. L. Myshkina, S. A. Yakovlev, I. I. Zharkova, A. L. Zernov, E. A. Filatova, D. V. Bagrov, A. V. Rebrov, G. A. Bonartseva, and A. L. Iordanskii, Chem. Chem. Technol. **6** (4), 385–392 (2012).

13. A. P. Bonartsev, A. L. Iordanskii, G. A. Bonartseva, and G. E. Zaikov, J. Balkan Tribol. Assoc. **14** (3), 359–395 (2008).

14. O. V. Staroverova, A. M. Shushkevich, G. M. Kuz'micheva, A. A. Ol'khov, V. V. Voinova, I. I. Zharkova, K. V. Shaitan, E. D. Sklyanchuk, and V. V. Gur'ev, Tekhnol. Zhivykh Sist. **10** (8), 74–79 (2013).

15. O. V. Staroverova, A. A. Ol'khov, G. M. Kuz'micheva, E. N. Domoroshchina, S. V. Vlasov, and Yu. N. Filatov, "Ultrathin fibers based on biopolymer polyhydroxybutyrate (PHB) modified with nanoscale modifications of titanium dioxide," Vestnik MITKhT **6** (6), 120–127 (2011).

16. A. A. Olkhov, O. V. Staroverova, G. M. Kuzmicheva, E. N. Domoroshina, Yu. N. Filatov, I. Yu. Filatov, S. V. Vlasov, A. L. Iordanskii, L. S. Shibryaeva, Yu. V. Tertishnaya, G. A. Bonartseva, A. P. Bonartsev, and G. E. Zaikov, "Nanofibrous materials on the basis of biopolymer—polyhydroxybutyrate," in *Nanostructured Polymers and Nanochemistry: Research Progress*, Ed. by A. K. Haghi, S. Kubica, and G. E. Zaikov, (IMPIB, Institute for Engineering of Polymer Materials and Dyes, Torun, Poland, 2012), pp. 25–36.

17. A. A. Ishchenko, S. G. Dorofeev, N. N. Kononov, and A. A. Ol'khov, RF Patent No. 2411613, Method for obtaining nanocrystalline silicon with a bright stable photoluminescence, Bull. No. 4 (February 10, 2011)

18. A. A. Ishchenko, V. N. Bagratashvili, N. N. Kononov, S. G. Dorofeev, and A. A. Ol'khov, RF Patent No. 2491227, Method for obtaining biodegradable nanosilicon particles for *in vivo* application, Bull. No. 24 (August 27, 2013).

19. S. G. Dorofeev, A. O. Rybaltovskii, A. A. Ishchenko, A. A. Krutikova, A. A. Ol'khov, N. N. Kononov, V. N. Bagratashvili, and N. V. Minaev, "Laser-induced effects in the Raman spectra of nanocrystalline silicon," Ross. Nanotekhnol. **7** (7), 96–101 (2012).
20. G. M. Kuz'micheva, E. V. Savinkina, L. N. Obolenskaya, et al., Kristallografiya **55** (5), 913–917 (2010).
21. A. A. Ol'khov, V. B. Ivanov, S. V. Vlasov, and A. L. Iordanskii, "Climatic aging of composite films based on LDPE and polyhydroxybutyrate (PHB)," Plast. Massy, No. 6, 19 (1998).
22. S. G. Karpova, A. L. Iordanskii, S. N. Chvalun, M. A. Shcherbina, S. M. Lomakin, N. G. Shilkina, S. Z. Rogovina, V. S. Markin, A. A. Popov, and A. A. Berlin, Dokl. Akad. Nauk **446** (5), 1–4 (2012).
23. *A Practical Course in Plastic Processing Technology,* Ed. by V. M. Vinogradov and G. S. Golovkin (Khimiya, Moscow, 1980) [in Russian].
24. A. I. Gusev, *Nanomaterials, Nanostructures, Nanotechnology*, 2nd ed. (FIZMATLIT, Moscow, 2009) [in Russian].
25. A. A. Ol'khov, O. V. Staroverova, Yu. N. Filatov, G. M. Kuz'micheva, A. L. Iordanskii, O. V. Stoyanov, G. E. Zaikov, and L. A. Zenitova, "Nanofibrous polyhydroxybutyrate-based biomaterials," Vestnik Kazan. Tekhnol. Univ. **16** (8), 157–161 (2013).
26. G. C. Rutledge and S. V. Fridrikh, Adv. Drug Delivery Rev., No. 14, 1384–1391 (2007).
27. M. L. Di Lorenzo, M. Gazzano, and M. C. Righetti, Macromolecules, 5684–5691 (2012).
28. A. A. Ishchenko, G. V. Fetisov, and L. A. Aslanov, *Nanosilicon: Properties, Production, Application, and Methods of Research and Monitoring* (Fizmatlit, Moscow, 2011) [in Russian].
29. A. A. Ishchenko and A. A. Ol'khov, RF Patent No. 2429189, Polymeric nanocomposite for protection against UV (September 20, 2011).
30. A. A. Ol'khov, D. Dzh. L'yao, G. V. Fetisov, M. A. Gol'dshtrakh, N. N. Kononov, A. A. Krutikova, P. A. Storozhenko, A. A. Ishchenko, "Nanocomposite films with UV-barrier properties based on polyethylene with ultrafine silicon," Plast. Massy, No. 9, 40–46 (2010).
31. A. A. Ishchenko, G. V. Fetisov, and L. A. Aslanov, *Nanosilicon: Properties, Production, Application, and Methods of Research and Monitoring* (FIZMATLIT, Moscow, 2011) [in Russian].
32. A. A. Popov, N. Ya. Rapoport, and G. E. Zaikov, *Oxidation of Oriented and Strained Polymers* (Khimiya, Moscow, 1987) [in Russian].
33. A. P. Boskhomdzhiev, A. P. Bonartsev, E. A. Ivanov, T. K. Makhina, V. L. Myshkina, D. V. Bagrov, E. V. Filatova, G. A. Bonartseva, A. L. Iordanskii, Int. Polym. Sci. Technol., No. 11, 25–30 (2010).

*Translated by O. Maslova*

SPELL: 1. ok